JOURNAL OF MATERIALS SCIENCE 24 (1989) 2437–2443

Continuous heating of rapidly solidified Al–Cr ribbons

KOJIRO F. KOBAYASHI, NOBUO TACHIBANA, PAUL H. SHINGU
Department of Metal Science and Technology, Kyoto University, Sakyo-ku, Kyoto 606, Japan

Rapidly solidified Al–Cr alloys have been prepared by a single roller method. Microstructures and the subsequent structural changes were examined as a function of alloy content and heat treatment. The phase transformation process of the ribbons at the continuous heating stage (0.33 K sec^{-1}) was determined by differential scanning calorimetry (DSC), X-ray diffraction analysis (XRD), scanning electron microscopy (SEM), and transmission electron microscopy (TEM). The precipitation temperature of θ in the supersaturated solid solution decreased with increasing degree of supersaturation, but that at the grain boundaries did not so greatly depend on the supersaturation.

1. Introduction

Rapid solidification is being extensively studied [1–3] as a means to increase the solid solubility of alloying elements, to refine microstructures, including grain size, and to obtain metastable phases. Rapidly solidified Al–Cr alloy is known to form metastable supersaturated solid solution in the range of lower chromium content and icosahedral quasicrystals over a wide composition range from about 5 to 16 at % Cr [4]. Al–Cr alloy is one of the most familiar materials and has been well investigated [4–16]. However, most previous studies [8–15] were limited to compositions of up to 2 at % Cr, except for a few reports [4–7, 16].

The purpose of this work was to investigate the characteristics of rapidly solidified Al–Cr ribbon, prepared by the single roller method, with compositions in the range 0 to 15 at % Cr. The decomposition process of the highly non-equilibrium state during the heating stage was detected by differential scanning calorimetry (DSC). The rapidly solidified structures and subsequent changes in the phase and morphology of the precipitates at each heating stage were examined by X-ray diffraction techniques (XRD), scanning electron microscopy (SEM) and transmission electron microscopy (TEM). The kinetics of equilibrium θ precipitates at the grain boundaries and within the matrix were extensively investigated.

2. Experimental procedure

Al–Cr binary alloys containing 2, 4, 6, 7, 10 and 15 at % Cr were used in the present work. Samples for rapid solidification were prepared by chill casting the alloys of desired composition, using 99.99% pure aluminium and 99.75% pure chromium, melting in an argon atmosphere in an alumina crucible. Rapidly solidified ribbons about 30 μm thick and about 2 mm wide were prepared using a single roller method [17] in an argon atmosphere. The amount of melted alloy per run was about 3 g and the surface speed of the wheel (α-brass) was about 42 m sec^{-1} to obtain well-shaped ribbons.

The thermal properties were examined in an argon atmosphere with DSC at a heating rate of 0.33 K sec^{-1}. The X-ray diffraction study was carried out using Cu$K\alpha$ radiation at room temperature.

Simultaneous measurements of diffraction peaks from powdered high-purity silicon were used as a standard. Electron microscopy (SEM and TEM) revealed the microstructure of the ribbon and its subsequent change during the heating stage which corresponded to the DSC curve. The TEM sample was prepared by thinning ribbons electrically in a solution of 10% perchloric acid and 90% ethyl alcohol at 273 K.

3. Results and discussion

3.1. Rapidly solidified ribbons

Fig. 1 shows TEM images of 2, 4, 6, 7, 10 and 15 at % Cr ribbons prepared by the single roller method (surface speed 42 m sec^{-1}). Fig. 2 shows X-ray diffraction patterns obtained from each ribbon. Ribbons of 2 at % Cr are a single phase where all the solute chromium dissolves in the aluminium matrix. X-ray analysis shows no existence of icosahedral quasicrystals for 4 at % Cr ribbon. However, TEM imaging clearly shows a spherical icosahedral phase (I phase) in the supersaturated solid solution. The volume fraction of I phase increases with increasing chromium content up to 15 at % Cr, and its morphology depends on the solute content. I phase is spherical in 4, 6 and 7 at % Cr, and the spherulites are characterized by elongated branches that stem from a centre core in 7 and 10 at % Cr; it degenerates into a featureless form in 15 at % Cr. Phases observed by X-ray diffraction, SEM and TEM studies in rapidly solidified ribbons (from the pure aluminium to Al–15 at % Cr) are listed in Table I.

0022–2461/89 $03.00 + .12

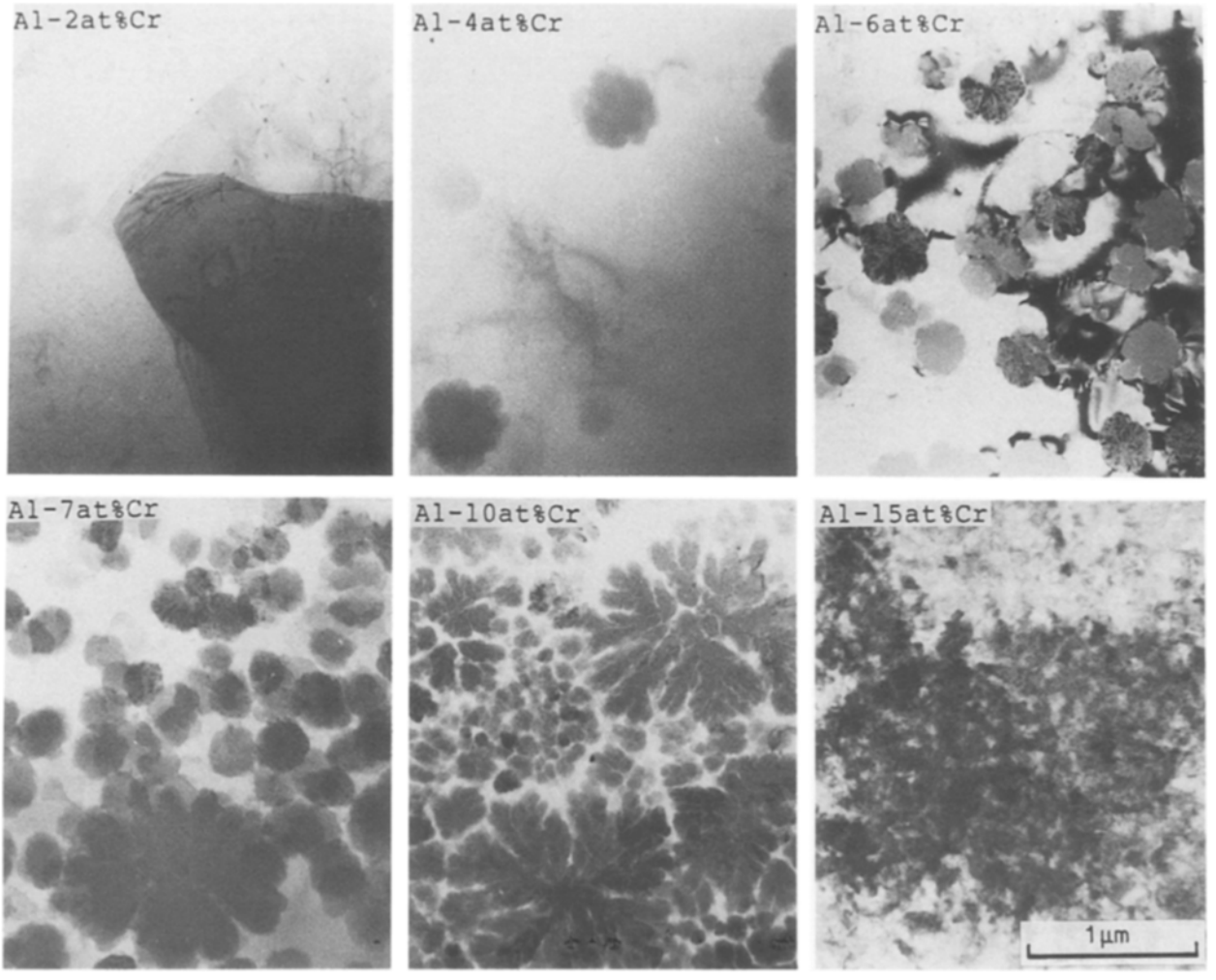

Figure 1 TEM images of Al–Cr ribbons prepared by the single roller method (surface speed 42 m sec^{-1}).

3.2. Processes of phase transformation

Electron microscopy and X-ray analysis reveal the microstructure of the ribbon and its subsequent change at each heating stage which corresponds to the DSC curve. Phases observed by SEM, TEM and X-ray studies (during continuous heating at the rate of 0.33 K sec^{-1}) are summarized in Fig. 3. All of the ribbons were prepared by the use of a brass wheel at a surface speed of 42 m sec^{-1}. For 15 at % Cr ribbon, this work could not completely characterize the phase change by crystallographic studies. The temperatures of the two exothermal peaks correspond well with those in a previous work [4] in which it was reported that the first and second peaks could be attributed to the transitions from quasicrystal to a metastable intermediate phase and from the intermediate phase to stable orthorhombic compound.

3.3. Extension of solid solubility

The lattice parameter of aluminium-rich phase is shown in Fig. 4 as a function of initial chromium content. It decreases with increasing chromium content up to about 6 at %, whereas the maximum equilibrium solid solubility is 0.37 at % Cr at 934 K [18]. King's relationship [19] calculated from the data in solid solution is also shown as a reference. The results have not been influenced by the roll surface speed (42 or 61 m sec^{-1}) and are about the same for the gun quenched sample [6, 20]. About 6 at % Cr is the maximum of the extended solid solubility.

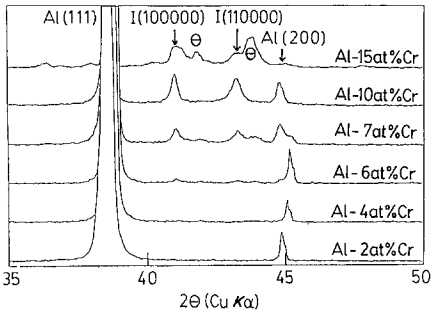

Figure 2 X-ray diffraction patterns of Al–Cr ribbons.

TABLE I Phases observed by X-ray diffraction, SEM and TEM studies in rapidly solidified Al–Cr ribbons prepared by the single roller method (surface speed 42 m sec^{-1})

	Observed phases
Al–2 at % Cr	Al(S.S.)
Al–4 at % Cr	Al(S.S.) (I)
Al–6 at % Cr	Al(S.S.) I
Al–7 at % Cr	Al(S.S.) Al I
Al–10 at % Cr	Al I
Al–15 at % Cr	I θ

S.S. = solid solution,
I = icosahedral phase.

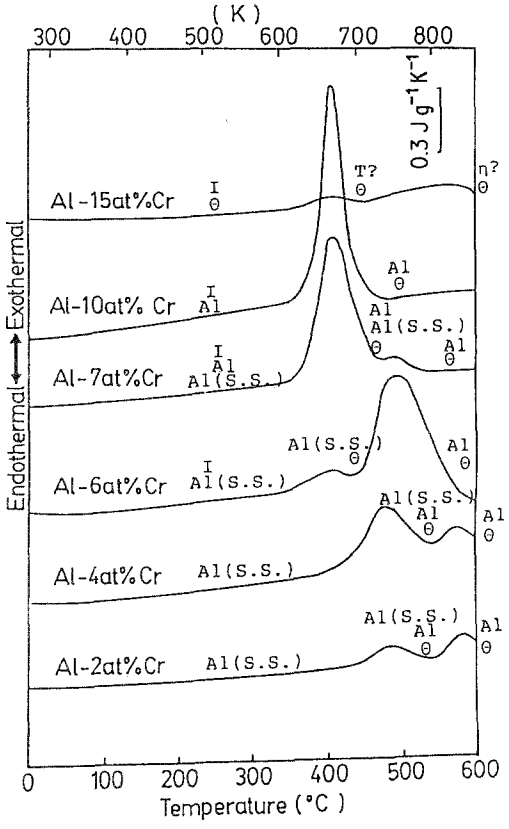

Figure 3 Phases observed by X-ray diffraction, SEM and TEM studies (in as-solidified and heat-treated Al–Cr ribbons) are shown in DSC curves. The DSC curves are taken during continuous heating at a rate of 0.33 K sec^{-1}. All of the ribbons were prepared using a brass wheel at a surface speed of 42 m sec^{-1}.

3.4. Decomposition of the supersaturated solid solution

3.4.1. Rapidly solidified Al–6 at % Cr ribbons

The maximum extended solid solubility was about 6 at % Cr. The solidification rate may be varied by controlling the surface speed of the wheel. Fig. 5 shows X-ray diffraction patterns of 6 at % Cr ribbons prepared at the different surface speeds of about 26, 42 and 61 m sec^{-1}. For three different speeds, the angles of supersaturated solid solution are about the same, although the phase and its volume fraction are different. The higher surface speed may result in a higher solidification rate, but 42 m sec^{-1} forms well-shaped ribbon in this study. Fig. 6 shows typical TEM images

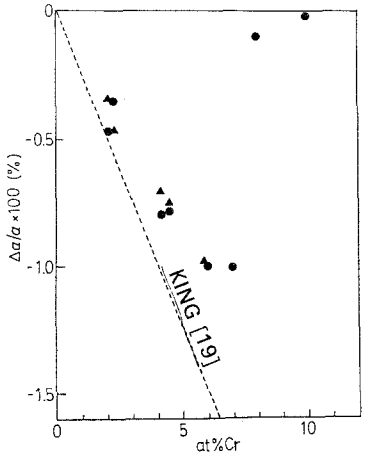

Figure 4 Lattice parameter of aluminium-rich phase as a function of initial chromium content. (●) 42 m sec^{-1}, (▲) 61 m sec^{-1}.

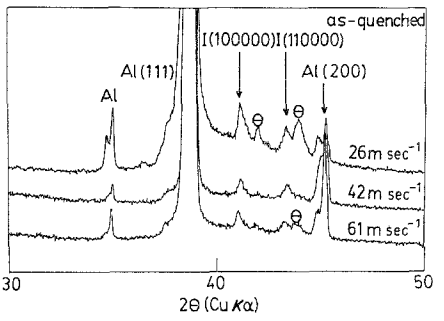

Figure 5 X-ray diffraction patterns of 6 at % Cr ribbons prepared at different surface speeds of 26, 42 and 61 m sec^{-1}.

of these ribbons. I phase is distributed in the supersaturated solid solution.

3.4.2. Continuous heating of Al–6 at % Cr ribbons

DSC curves during continuous heating at the rate of 0.33 K sec^{-1} are shown in Fig. 7. The first peak corresponds to the phase change of I phase to equilibrium θ. The second and third peaks (61 m sec^{-1}) correspond to the decomposition of supersaturated solid solution for θ precipitation; 26 m sec^{-1} is not significantly different from 42 m sec^{-1}.

X-ray diffraction patterns of as-solidified and heat-treated ribbons for 42 and 61 m sec^{-1} are shown in Figs 8 and 9, respectively. TEM images of the ribbons and their subsequent changes during the heating stage are shown in Figs 10 and 11 for 42 and 61 m sec^{-1}, respectively. Spherical I phase formed during solidification changes into a mixed structure of α and θ after the first peak (at 713 K in Fig. 10, at 693 K in Fig. 11). Temperatures shown in figures correspond to the DSC curves. Fig. 11 indicates that the precipitation of θ at grain boundaries and in the matrix produces the second and third peaks of the DSC curve, respectively. This tendency of two-step precipitation is observed in the lower chromium content ribbons as seen in Fig. 3.

3.4.3. Precipitation of θ from supersaturated solid solution

Precipitation along the grain boundaries occurs at temperatures lower than those which produce precipitation within the grain boundaries. These temperatures are strongly dependent on the chromium content in solid solution. Fig. 12 shows the relationship between precipitation temperature and lattice parameter of the aluminium-rich phase, where lines represent the peak temperatures of precipitation along the grain boundaries (GBP) and in the matrix (MP) at the continuous heating rate of 0.33 K sec^{-1}. The temperature of MP decreases with increasing degree of supersaturation of the solid solution but that of GBP does not depend so much on the supersaturation.

The activation energy of θ precipitation for Al–6 at % Cr (62 m sec^{-1}) is measured by changes in the peak temperature due to the changes in the heating rates (0.083, 0.17, 0.33 K sec^{-1}). By the application of Kissinger's analysis [21], the apparent activation energies are determined as 2.2 eV for GBP and 4.9 eV for MP. As the activation energy of chromium diffusion

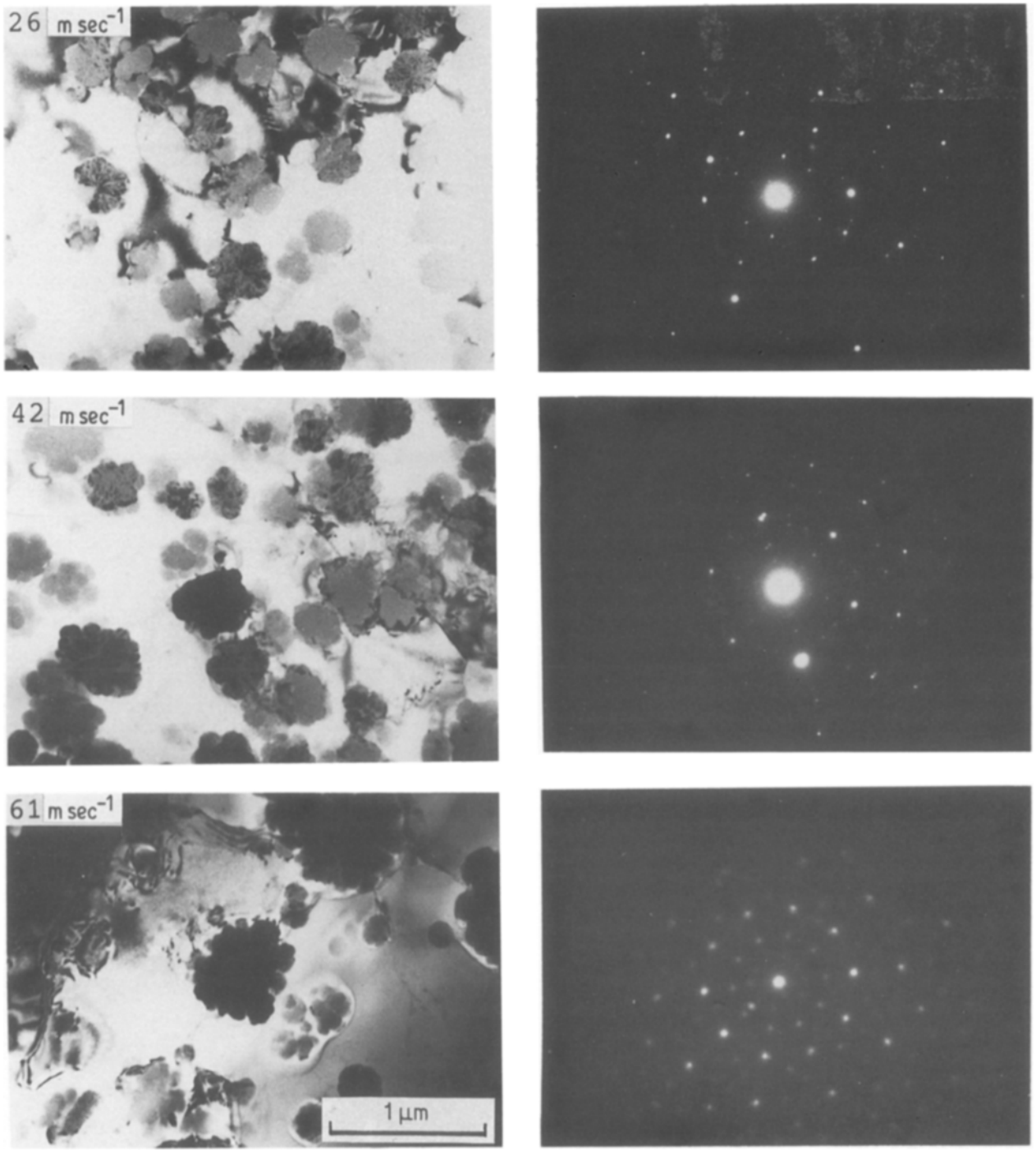

Figure 6 Typical TEM images of 6 at % Cr ribbons prepared at different surface speeds of 26, 42 and 61 m sec^{-1}.

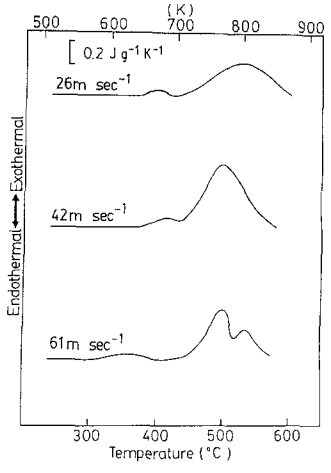

Figure 7 DSC curves of 6 at % Cr ribbons during continuous heating at a rate of 0.33 K sec^{-1}.

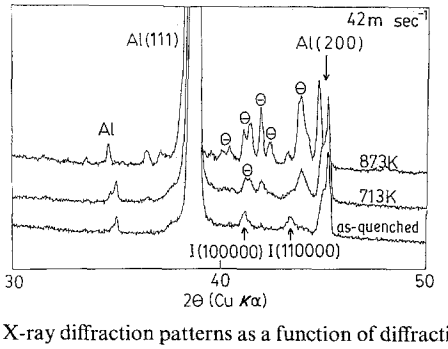

Figure 8 X-ray diffraction patterns as a function of diffraction angle for 6 at % Cr ribbons (surface speed 42 m sec^{-1}): as-solidified and quenched from each heating temperature. The temperature corresponds to the DSC curve.

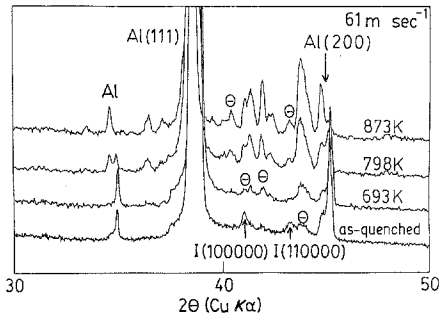

Figure 9 X-ray diffraction patterns as a function of diffraction angle for 6 at % Cr ribbons (surface speed 61 m sec^{-1}): as-solidified and quenched from each heating temperature. The temperature corresponds to the DSC curve.

in aluminium solid is 2.5 eV [22], these measured values seem to be reasonable.

4. Conclusions

Rapid solidification of Al–Cr alloys, with compositions in the range 0 to 15 at %, has been carried out using a single roller method. The structure and its subsequent changes in phase were evaluated both on the as-solidified and after heat treatments. The main results are summarized as follows.

1. The lattice parameter of aluminium decreased with increasing chromium content up to about 6 at %.

2. The icosahedral phase formed during solidification was spherical in 4, 6 and 7 at % Cr, and the spherulites

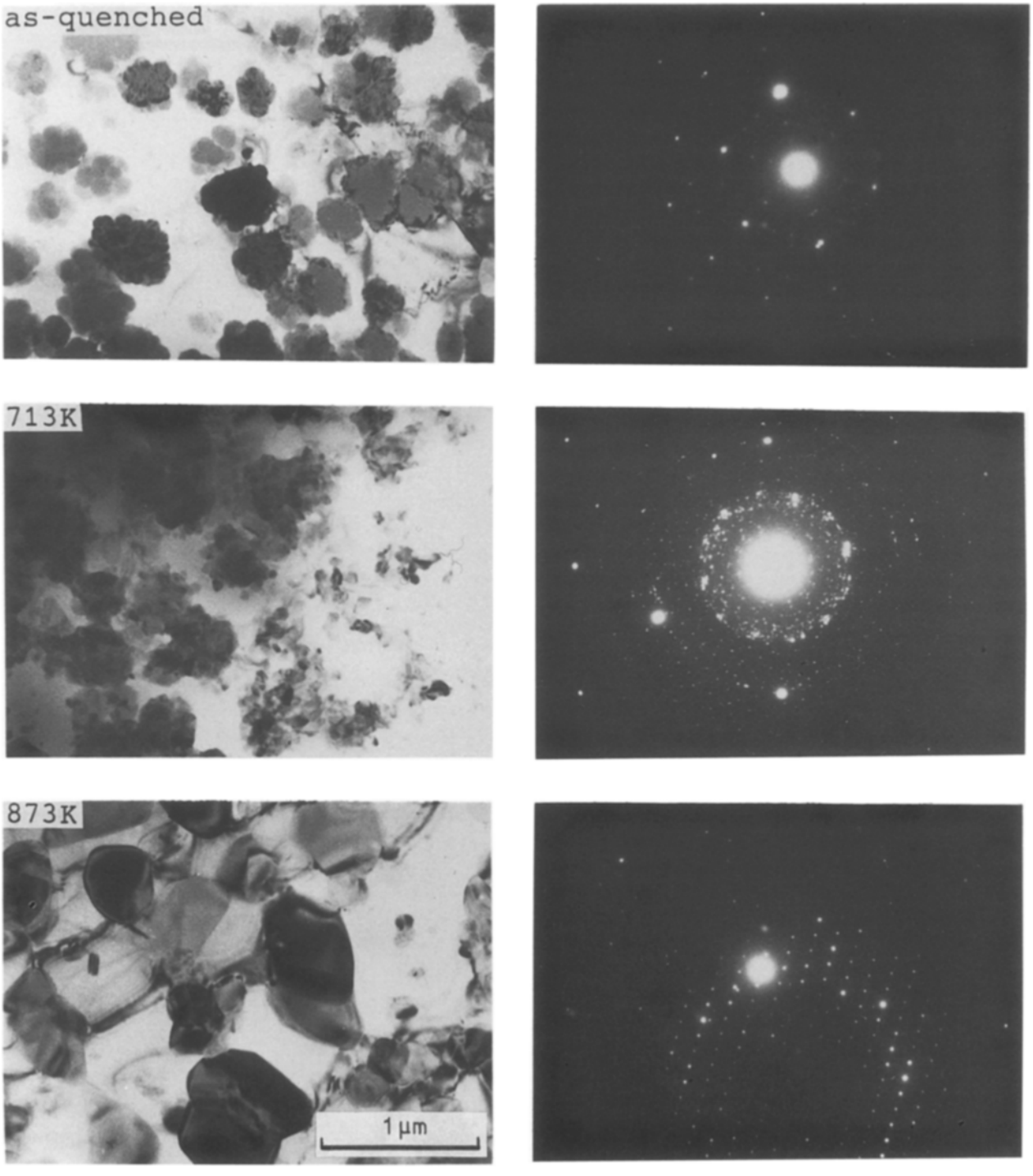

Figure 10 TEM images of 6 at % Cr ribbons (surface speed 42 m sec^{-1}) showing the changes of the rapidly solidified structures during continuous heating at a rate of 0.33 K sec^{-1}.

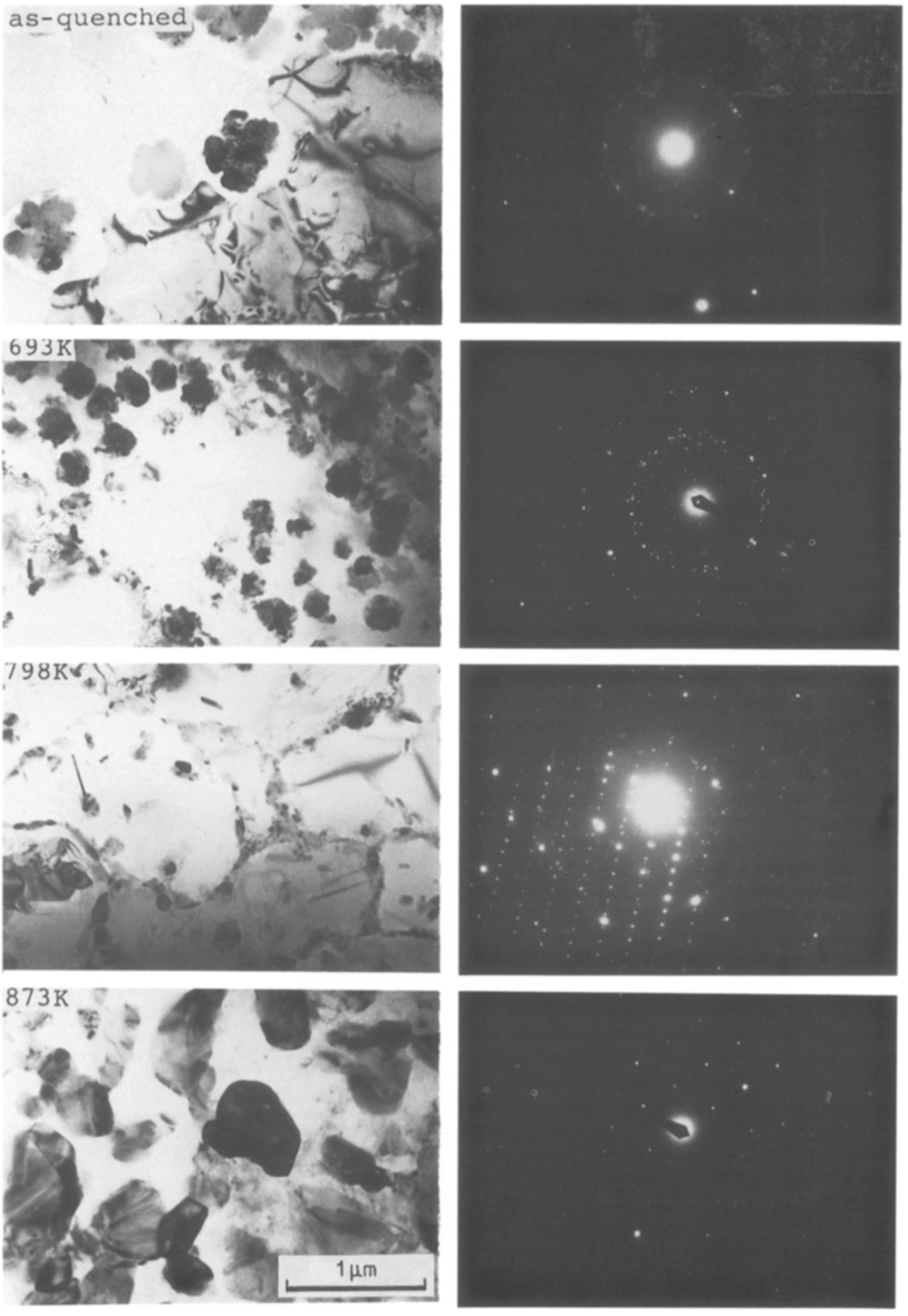

Figure 11 TEM images of 6 at % Cr ribbons (surface speed 61 m sec^{-1}) showing the changes of the rapidly solidified structures during continuous heating at a rate of 0.33 K sec^{-1}.

were characterized by elongated branches that stemmed from a centre core in 7 and 10 at % Cr. They became featureless in 15 at % Cr.

3. The decomposition process of the ribbons on continuous heating (0.33 K sec^{-1}) was determined by DSC, X-ray diffraction, SEM and TEM.

4. The precipitation temperature of θ in the α matrix (MP) decreased with increasing degree of

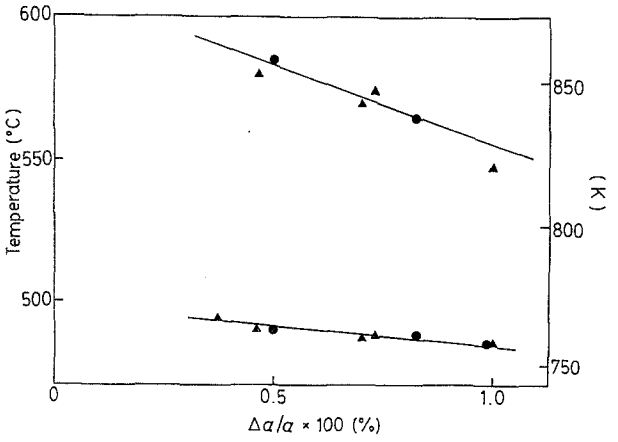

Figure 12 Precipitation temperatures of θ at the grain boundaries (GBP) and in the matrix (MP) shown as a function of the degree of supersaturation. (●) 42 m sec^{-1}, (▲) 61 m sec^{-1}.

supersaturation of the solid solution (α) but that at the grain boundaries (GBP) did not depend so greatly on the supersaturation.

References

1. T. R. ANANTHARAMAN and C. SURYANARAYANA, *J. Mater. Sci.* **6** (1971) 1111.
2. H. JONES and C. SURYANARAYANA, *J. Mater. Sci.* **8** (1973) 705.
3. B. H. KEAR and B. C. GIESSEN (eds), "Rapidly Solidified Metastable Materials" (North-Holland, New York, 1984) p. 3.
4. A. INOUE, H. KIMURA and T. MASUMOTO, *J. Mater. Sci.* **22** (1987) 1758.
5. S. P. MIDSON, R. A. BUCKLEY and H. JONES, "Proceedings of the 4th International Conference on Rapidly Quenched Metals", edited by T. Matsumoto and K. Suzuki (Japan Institute of Metals, Sendai, 1982) p. 1521.
6. H. WARLIMONT, W. ZINGG and P. FURRER, *Mater. Sci. Engng* **23** (1976) 101.
7. P. FURRER and H. WARLIMONT, *ibid.* **28** (1977) 127.
8. H. JONES, "Rapid Solidification Processing, Principles and Technology II", edited by R. Mehrabian, B. Kear and M. Cohen (Claitor's, Baton Rouge, 1980) p. 306.
9. R. ICHIKAWA, T. OHASHI and T. IKEDA, *Trans. Jpn Inst. Metals* **12** (1971) 280.
10. N. I. VARICH and R. B. LYUKEVICH, *Russ. Metall.* **4** (1970) 58.
11. A. F. POLESYA and A. I. STEPINA, *Phys. Metal Metallogr.* **27** (1969) 122.
12. V. I. DOBATKIN, V. I. ELAGIN, V. M. FEDOROV and R. M. SIZOV, *Izv. Acad. Nauk Metall.* **2** (1970) 199.
13. R. ICHIKAWA and I. OHASHI, *J. Jpn Inst. Metals* **34** (1970) 115.
14. T. OHASHI and R. ICHIKAWA, *ibid.* **34** (1970) 356.
15. K. NAGAHAMA and I. MIKI, *Trans. Jpn Inst. Metals* **15** (1974) 185.
16. L. BENDERSKY, R. J. SCHAEFER, F. S. BIANCANIELLO and D. SHECHTMAN, *J. Mater. Sci.* **21** (1986) 1889.
17. K. F. KOBAYASHI, T. AWAZU and P. H. SHINGU, *J. Mater. Sci. Lett.* **6** (1987) 781.
18. M. HANSEN and K. ANDERKO (eds), "Constitution of Binary Alloys" (McGraw-Hill, New York, 1958) p. 110.
19. H. W. KING, *J. Mater. Sci.* **1** (1966) 79.
20. P. FURRER and H. WARLIMONT, *Z. Metallkde.* **62** (1971) 100.
21. H. E. KISSINGER, *Anal. Chem.* **29** (1957) 1702.
22. N. L. PETERSON and S. J. ROTHMAN, *Phys. Rev.* **31** (1970) 3264.

Received 17 May
and accepted 12 September 1988